RSC Advances

ROYAL SOCIETY OF CHEMISTRY

www.rsc.org/advances

Table of Contents Entry

GRAPHIC

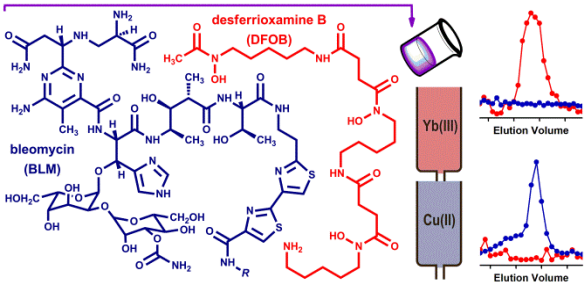

TEXT

A solution of bleomycin (BLM) and desferrioxamine B (DFOB) was resolved using two in-series columns containing BLM- or DFOB-tailored IMAC resin as a method with potential for accessing multiple clinical agents from fermentation

Journal Name

RSCPublishing

ARTICLE

The resolution of two clinical agents, bleomycin and desferrioxamine B, from a *Streptomyces verticillus* fermentation mixture using multi-dimensional immobilised metal ion affinity chromatography

Cite this: DOI: 10.1039/x0xx00000x

Received 00th January 2012,
Accepted 00th January 2012

DOI: 10.1039/x0xx00000x

www.rsc.org/

J. Gu and R. Codd

The multi-step process of extracting and purifying secondary metabolites as pharmaceutics from bacterial culture often represents the highest overall cost in production, and can require large volumes of organic solvents. In this work, we describe an aqueous-compatible, streamlined and selective method for the simultaneous isolation of two clinical agents, bleomycin (BLM) and desferrioxamine B (DFOB), from a standard solution, and from native *Streptomyces verticillus* culture. The method used two in-series columns containing immobilised metal ion affinity chromatography (IMAC) resin charged with Yb(III) (upper column) or Cu(II) (lower column), designed to exploit differences between the coordination chemistry of DFOB and BLM. Application of this multi-dimensional (MD)-IMAC configuration to a standard solution containing DFOB and BLM resulted in a complete resolution, with the high-yielding (~90%) isolation of DFOB on the Yb(III)-charged resin, and BLM on the Cu(II)-charged resin. The resolution was dependent upon the metal ion, the denticity of the immobilised chelate and the column order. The method was successful in the complete resolution of native DFOB and BLM from the complex *S. verticillus* fermentation mixture. DFOB eluted from the Yb(III) resin as the free ligand. BLM eluted from the Cu(II) resin as BLM A_2, Cu(II)-BLM A_2 and Cu(II)-BLM B_2. The optimised Yb(III)-IMAC format had a DFOB binding capacity (≥95%) of 8 μmol mL^{-1}, which is significantly greater than previously described formats. This work has demonstrated the potential of MD-IMAC for improved pharmaceutics processing of agents from fermentation through process intensification, and for reducing the environmental, occupational and financial costs of the use of organic solvents.

1. Introduction

Immobilised metal ion affinity chromatography (IMAC) was developed in the mid-1970s for the purification of native and recombinant histidine-tagged (His-tag) proteins.[1-4] The IMAC format comprises an insoluble matrix with an immobilised ligand (e.g., iminodiacetic acid, IDA) coordinated to a metal ion (e.g., Ni(II)) in an unsaturated fashion. The His-tag protein is retained on the resin *via* the formation of coordinate bonds between the imidazole side chains and the vacant sites of the Ni(II)-IDA complex, with target displacement effected by ligand competition (e.g., imidazole) or by a reduction in the pH value (pK_a IDA < pH < pK_a imidazole).

While the original application of IMAC remains ubiquitous in molecular biology, the method has been used more recently to isolate non-protein, low-molecular-weight metabolites from bacterial culture that have an inherent affinity and/or a functional requirement for binding selected metal ions.[5-9] Bacterial secondary metabolites form the major source of clinical agents for treating infection and cancers.[10-16] The ongoing need to discover new drugs produced by bacteria and other natural sources is coupled to developments in separation science. Improved purification methods can progress small-scale drug discovery programs through the isolation of low-abundant metabolites, and large-scale pharmaceutics production through increased efficiency. Methods that reduce the reliance on organic solvents are particularly favourable for reasons of reduced environmental impact and improved workplace safety.[17-21]

In this work, we demonstrate the use of a separation method termed multi-dimensional (MD)-IMAC,[9] designed to simultaneously isolate more than one non-protein, low-molecular-weight clinical agent from a single solution. The MD-IMAC format features two in-series columns containing IMAC resin tailored towards selecting different target

metabolites from the solution or mixture. MD-IMAC offers three potential benefits to Green pharmaceutics processing: (i) process intensification through isolating multiple agents from a single mixture; (ii) improved purification factors compared to columns configured in parallel; and (iii) water compatibility.

This work focusses upon two clinically-relevant agents: desferrioxamine B (DFOB), which is a high-Fe(III)-affinity bacterial siderophore used for treating transfusion-dependent iron overload disease,[22] and bleomycin (BLM), which is a class of antitumor antibiotics used to treat testicular, skin, head and neck cancers, and Hodgkin's lymphoma (Scheme 1).[23-25] IMAC has been used previously to isolate DFOB or BLM as single agents from cultures of DFOB-producing *Streptomyces pilosus* (Ni(II)-charged IDA resin, binding capacity 3 μmol mL^{-1})[5] or BLM-producing *Streptomyces verticillus* (Cu(II)-charged IDA resin, binding capacity 0.15-0.3 μmol mL^{-1}).[6] Here, we have examined the potential of MD-IMAC to resolve a solution of DFOB and BLM, as prepared from standards; or from the complex secondary metabolome of *S. verticillus*.

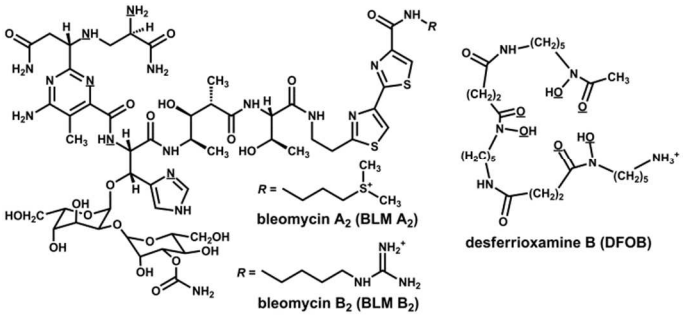

Scheme 1 Structures of bleomycin (BLM) congeners (BLM A_2, BLM B_2) and desferrioxamine B (DFOB), which are isolated for clinical use from fermentation mixtures. The functional groups for coordinating metal ions, as essential for their mechanisms of action, and potential for isolation using IMAC, are underlined.

2. Experimental

2.1. Materials

Chemicals were used as received, as sourced from Sigma-Aldrich: NaCl (99%), imidazole (≥99%), $Yb(NO_3)_3{\cdot}5H_2O$ (100%), $Fe(ClO_4)_3$, $Ga(NO_3)_3{\cdot}9H_2O$ (99.9%), $In(NO_3)_3{\cdot}H_2O$ (99.9%), desferrioxamine B mesylate (DFOB, 95%); Astral Scientific: 4-(2-hydroxyethyl)piperazine-1-ethanesulfonic acid (HEPES, 99%), $Na_2EDTA{\cdot}2H_2O$ (99%); Ajax Finechem: $NaH_2PO_4{\cdot}2H_2O$ (>98%), $CuSO_4{\cdot}5H_2O$ (98%); Merck: Na_2HPO_4 (>99%); and BioAustralis: bleomycin complex (as sulfate salts, >99%). Additional chemicals for preparing bacteriological medium were from Sigma-Aldrich: peptone, soybean flour, corn starch, glucose, K_2HPO_4 (>98%) and $ZnSO_4{\cdot}7H_2O$. Resins/columns were from GE Healthcare: His GraviTrap affinity columns, containing 1 mL of Ni(II)-charged IDA resin; Qiagen: Ni(II)-charged NTA superflow resin, 5-mL polypropylene columns; or Roche: Ni(II)-charged cOmplete His-Tag purification resin (Ni(II)-charged COM), metal-free cOmplete His-Tag purification resin (COM). The frozen permanents of *S. verticillus* ATCC 15003 were kept in DMSO at –80°C, as described previously.[6]

2.2. Instrumentation

Measurements of pH were made using a Microprocessor pH meter (Model: pH 211) with a 5-mm glass pH electrode (Model: H1 1330) from Hanna instruments. Absorbance values were obtained from solutions in 96-well plates on a FluoStar plate reader or PolarStar plate reader. Liquid chromatography-mass spectrometry (LC-MS) measurements were conducted on an Agilent series 1200 LC system with an Agilent 1260 Infinity binary pump with integrated vacuum degasser, autosampler, thermostated column compartment and diode array detector, and an Agilent 1260 quadrupole mass spectrometer. The capillary voltage was 3 kV. Total ion monitoring mass range was from 100 to 1500. Samples were processed using an Eclipse XDB-C18 column (Agilent; particle size: 5 μM; column dimensions: 150 mm × 4.6 mm i.d.) under the following conditions: linear gradient of 0-28% B (A: 100% H_2O/0.1% formic acid; B: 100% acetonitrile (ACN)/0.1% formic acid) over 20 min, a flow rate of 0.5 mL min^{-1} and an injection volume of 10 μL. Selected ion monitoring (SIM) was used at the specified *m/z* values. Agilent OpenLAB Chromatography Data System (CDS) ChemStation Edition was used for data acquisition and processing.

2.3. Preparation and analysis of solutions of DFOB and BLM

The following buffers were prepared: high-pH binding buffer (high-pH BB, 25 mM HEPES, 0.5 M NaCl, pH 9.0), low-pH elution buffers (25 mM HEPES, 0.5 M NaCl, at pH 4.0 (low-pH-4 EB) or pH 5.0 (low-pH-5 EB)); and phosphate buffer (20 mM NaH_2PO_4/Na_2HPO_4, 0.5 M NaCl, pH 8.0). Solutions of DFOB or BLM (5 mM, 2.5 mM, 1.25 mM, 0.625 mM, 0.313 mM, 0.156 mM, 0.078 mM, 0.039 mM, 0.020 mM) were prepared from stock solutions in high-pH BB or low-pH-4 or low-pH-5 EB. Aliquots (200 μL) of the DFOB solutions were transferred into a 96-well plate and were mixed with 100 μL of ferric assay solution (10 mM $Fe(ClO_4)_3$ in 0.2 M $HClO_4$). The absorbance value at 470 nm was measured after 10 min incubation time. Aliquots (200 μL) of the BLM were transferred into a 96-well plate and the absorbance value at 290 nm was measured.

2.4. Preparation of IMAC resins

HisGraviTrap affinity columns (Ni(II)-IDA resin, 1 mL) were used as received. For metal ion exchange, the resin was washed with EDTA solution (5 mL), phosphate buffer (5 mL), and water (5 mL); and re-charged with Cu(II), Yb(III), Ga(III) or In(III), by washing the resin with an aqueous solution (0.1 M, 0.5 mL) of the corresponding metal ion. To remove excess metal ions, the resin was washed with 0.25 M imidazole, 0.3 M NaCl, 50 mM NaH_2PO_4/Na_2HPO_4, pH 8.0 (5 mL), Milli-Q water (5 mL) and 20 mM NaH_2PO_4/Na_2HPO_4, 0.5 M NaCl, pH 8.0) (5 mL). The Ni(II)-charged or metal-free COM resin was packed into a polypropylene column (final bed volume, 1 mL). The metal-free COM resin was charged with Yb(III) and the

resin was treated to remove unbound metal ions, as described above. The Ni(II)-charged NTA resin was packed into a polypropylene column (final bed volume, 1 mL) and the Ni(II) was exchanged for In(III), as described above. All columns were equilibrated with 5 mL high-pH BB prior to sample loading.

2.5. Conducting IMAC and MD-IMAC experiments

For each IMAC experiment, an aliquot (250 µL) of DFOB (10 mM or 0.625 mM) or BLM (0.625 mM), or a mixture of DFOB and BLM (0.625 mM DFOB and 0.625 mM BLM), were adsorbed onto the column assembly. For single-column IMAC experiments, the column was washed with 4 mL of high-pH BB followed by 4 mL of low-pH-5 EB or 4 mL of low-pH-4 EB for Yb(III)-COM systems. Fractions (250 µL) were assayed for DFOB or BLM, as described above. Sample loadings and conditions for each MD-IMAC experiment were as stipulated in Table 2.

2.6. Bacterial culture of *Streptomyces verticillus*

Streptomyces verticillus ATCC 15003 was cultured according to literature methods.[6,26,27] The strain was initially cultured in a pre-culture medium (100 mL) comprised of (w/v) 0.75% peptone, 0.75% soybean flour, 1.0% corn starch, 1.0% glucose and 0.3% NaCl (medium pH 6.5-7.0). To inoculate cells, 1 mL of the frozen permanent stock of *S. verticillus* was pipetted into the sterile medium. The pre-culture was grown at 28 °C on an orbital shaker at 220 rpm for 48 h. The final culture was grown in medium consisting of 3.5% soybean flour, 2.5% corn starch, 0.5% glucose, 0.05% $ZnSO_4 \cdot 7H_2O$, 0.01% $CuSO_4 \cdot 5H_2O$ and 0.1% K_2HPO_4 (medium pH 6.5-7.0). The final culture was grown for 10 days under the same conditions as the pre-culture. After 10 days, the cells were centrifuged for 50 min at 4000 rpm to collect the supernatant. The supernatant was subject to purification on XAD-2 resin as previously described[6] to remove Cu(II) from any BLM that was present as Cu(II)-BLM. Fractions containing Cu(II)-free BLM were pooled and were concentrated using rotary evaporation, and freeze dried.

2.7. MD-IMAC of *S. verticillus* culture

The freeze-dried powder (170 mg) was re-dissolved in 1.0 mL of high-pH BB and diluted to 1:2 and 1:4 of the original concentration. The concentration of BLM and DFOB in the native culture was estimated as 10 mg L^{-1} and 0.05 mg L^{-1}, respectively. Equal volumes of these solutions were combined and an aliquot (250 µL) of this solution was adsorbed onto the two-column assembly (Yb(III)-charged COM (upper); Cu(II)-IDA (lower)) and washed with 4 mL of high-pH BB. The columns were disassembled and each column was washed with the appropriate low-pH EB. Fractions (250 µL) were analysed for BLM and DFOB using LC-MS with modes of detection as stipulated in the main text.

3. Results and discussion

3.1. Opening comments

BLM and analogues are currently extracted from fermentation mixtures using methanol or *n*-butanol, with downstream chromatography using methanol or acetone as solvents.[27-29] DFOB and analogues have been purified using different protocols, including multiple recrystallizations from water-methanol,[30] recovery from macro-reticular resins upon elution with water-acetonitrile-methanol,[31] and extraction as Fe(III) complexes into benzyl alcohol or chloroform-phenol.[32-34] The simultaneous isolation of DFOB and BLM using a protocol with a small number of steps and a reduced reliance on the use of organic solvents could have potential for Green pharmaceutics processing.

Since DFOB and BLM have different affinities towards a range of metal ions (Table 1), it was thought that a judicious selection of metal ions in an MD-IMAC format could enable the concentration of each agent on individual IMAC columns (Scheme 2a). A modest difference between the affinity of DFOB or BLM for a given metal ion would compromise the resolution (Scheme 2b,c).

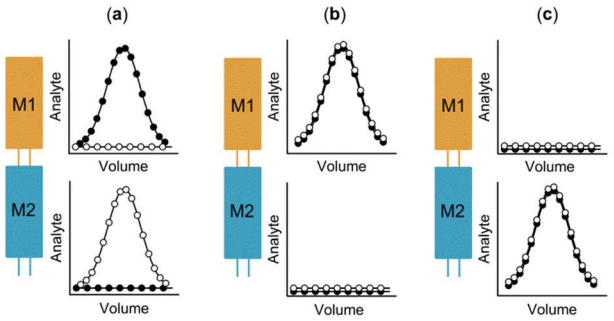

Scheme 2 A mixture of two analytes (A1, solid; A2, open) processed on two in-series columns containing IMAC resin charged with different metal ions (M1, upper; M2, lower) could potentially result in each analyte being concentrated on a separate column, affording complete resolution (**a**); or both analytes being concentrated on the same column, affording no resolution (upper, **b**; lower, **c**).

In the MD-IMAC experiments, a solution containing equimolar DFOB and BLM in high-pH binding buffer (high-pH BB, pH 9.0), was adsorbed onto the two-column assembly. After sample loading, the assembly was washed with a defined volume of high-pH BB to elute unbound components. The columns were then disassembled and were washed separately with a defined volume of low-pH elution buffer (low-pH EB at pH 4.0 or pH 5.0). The wash with low-pH EB was designed to reverse the target ligand-metal binding, due to protonation of the coordinating functional groups (Scheme 1), but not to dissociate the metal-IDA binding (IDA, pK_{a1} 1.8; pK_{a2} 2.6).[35] Fractions were analysed for DFOB using an Fe(III) addition assay (λ_{max} 470 nm),[36] and for BLM using UV absorbance (λ_{max} 290 nm) (see Fig S1 in ESI†). In some experiments, selected fractions were analysed using LC-MS to improve detection limits, and to inform whether DFOB or BLM was eluted as the free ligand and/or a coordination complex.

3.2. MD-IMAC for the resolution of BLM and DFOB from a standard solution: initial experiments

Since Ni(II)- or Cu(II)-charged IDA resin has been shown to effectively retain DFOB or BLM, respectively, these resin types were first examined in a MD-IMAC format, with the column containing the Ni(II)-charged IDA resin mounted above the column containing the Cu(II)-charged IDA resin. Similar to previous single-column IMAC experiments, DFOB was captured on the Ni(II)-charged IDA resin (Fig. 1a) in 90% yield (Table 2, Run 1). BLM did not bind to the lower-positioned Cu(II)-charged IDA resin, but instead eluted from the two-column assembly during the high-pH BB wash (Fig. 1a,b). LC-MS measurements showed the presence of Ni(II)-BLM A_2 ($[Ni(II)\text{-}M]^{2+}$, m/z_{calc} 735.7, m/z_{obs} 735.7 (9.7%); $[Ni(II)\text{-}M + H^+]^{3+}$, m/z_{calc} 490.8, m/z_{obs} 491.0 (62.2%); $[Ni(II)\text{-}M + 2H^+]^{4+}$, m/z_{calc} 368.4, m/z_{obs} 368.6 (100%)) and Ni(II)-BLM B_2 ($[Ni(II)\text{-}M]^{2+}$, m/z_{calc} 741.2, m/z_{obs} 741.2 (16.1%); $[Ni(II)\text{-}M + H^+]^{3+}$, m/z_{calc} 494.5, m/z_{obs} 494.7 (74.9%); $[Ni(II)\text{-}M + 2H^+]^{4+}$, m/z_{calc} 371.1, m/z_{obs} 371.3 (100%)), which indicated that BLM was leaching Ni(II) from the Ni(II)-IDA complex, and as a metal complex was no longer a competent IMAC ligand. Reversal of the column order (Cu(II)-charged IDA resin (upper), Ni(II)-charged IDA resin (lower)) was ineffective in resolving DFOB and BLM, with the major fraction of both analytes binding to the upper-positioned Cu(II)-charged IDA resin (Fig. 1d). This observation was in accord with the significant affinity of 1:1 complexes between Cu(II) and DFOB (log*K* 14.1) or BLM (log*K* 12.6), and demonstrated that column order would likely be a significant determinant of analyte resolution.

Table 1 Log*K* values of 1:1 complexes formed between selected metal ions and analytes DFOB or BLM, or IMAC-relevant polyaminocarboxylic acid chelates or analogues

Ligand	Log*K*[a,b]		
	Ni(II)	Cu(II)	Yb(III)
DFOB	10.9[c]	14.1[c]	16.0[c]
BLM[d]	11.3[c,e]	12.6[c,e]	NA[f]
IDA	8.1	10.6	7.4
NTA[g]	11.5	12.9	12.2
BEDTRA[h]	NA[f]	16.8[i]	13.9[j]
EDTA[k]	18.5	18.7	19.5

[a] 25 °C, 0.1 M (unless otherwise specified). [b] From Refs 37,38 (unless otherwise specified). [c] 20 °C, 0.1 M. [d] For congener BLM-A_2. [e] From Ref 39. [f] NA, not available. [g] NTA, nitrilotriacetic acid. [h] BEDTRA, *N*′-benzylethylenediamine-*N*,*N*,*N*′-triacetic acid. [i] From Ref 40. [j] From Ref 41. [k] EDTA, ethylenediamine-*N*,*N*,*N*′,*N*′-tetraacetic acid.

Since DFOB has an affinity towards a wide range of transition metal ions,[42,43] the most effective MD-IMAC design would select for DFOB in the upper-positioned column to reduce competition against BLM for binding sites on the lower-positioned IMAC column. Metal ions, including Fe(III) and Ga(III), that form high-affinity complexes with DFOB (log*K* 31.0 and log*K* 28.2, respectively),[44] were not suitable in an IMAC format for DFOB capture, since DFOB leached the metal ion from the immobilised complex.[9] Ytterbium(III)-charged IDA resin was posited as a metal ion with potential for retaining DFOB, based on the log*K* value (Table 1). Further, a Yb(III)-charged IMAC matrix would likely select for DFOB above BLM, since based on the hard and soft acids and bases (HSAB) theory,[45,46] the five N-based donor groups in BLM would predict for reduced affinity to this hard lanthanide metal ion. The isolation of proteins using Yb(III)-charged IMAC resins has previously been examined,[47,48] but this is the first study of Yb(III)-based IMAC for the capture of non-protein, low-molecular-weight bacterial secondary metabolites.

An MD-IMAC experiment conducted with Yb(III)-charged IDA resin in the upper-positioned column and Cu(II)-charged IDA resin in the lower-positioned column showed a significant but incomplete resolution of DFOB and BLM (Fig. 2a,b, Table 2, Run 2). The majority of DFOB was concentrated on the Yb(III)-charged IDA resin (79%), with a smaller fraction binding to the Cu(II)-charged IDA resin (20%). The majority of BLM (88%) passed through the Yb(III)-charged IDA resin and was retained on the lower-positioned Cu(II)-charged IDA resin. Key to this partial resolution was the differential binding affinities of DFOB or BLM towards Yb(III). In effect, the Yb(III)-charged IDA resin was acting as a pre-column to remove DFOB from the solution to reduce competition between DFOB and BLM for the binding sites on the Cu(II)-IDA resin.

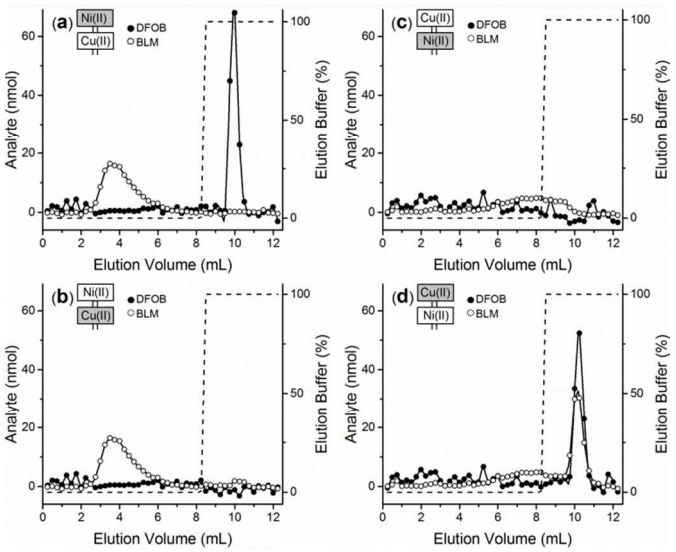

Fig. 1 The resolution profile of DFOB (closed circles) and BLM (open circles) upon processing an aliquot (250 µL) of an equimolar solution of DFOB and BLM (156 nmol:156 nmol) on two columns configured in series, which contained 1 mL of IMAC resin charged with Ni(II) (upper column, IDA resin) or Cu(II) (lower column, IDA resin) (**a**, **b**); or Cu(II) (upper column, IDA resin) or Ni(II) (lower column, IDA resin) (**c**, **d**). Analyte concentrations were measured in the fractions eluted with high-pH binding buffer from the two-column assembly, and from the individual columns with low-pH-5 elution buffer after disassembly (Ni(II), **a**, **c**; Cu(II), **b**, **d**). The gradient is shown as the broken line.

As a measure of the efficiency of a given type of resin to capture DFOB or BLM, a performance factor (PF) was defined by Equation 1, where A1 was set as the analyte captured in higher concentration, and A2 was the other analyte. The first term in brackets provides a measure of resolution (e.g., for Run 2: Yb(III)-IDA_{DFOB} = (1 – 0/79) = 1; and Cu(II)-IDA_{BLM} = (1 – 20/88) = 0.77). The second term in brackets represents a measure of capacity, as the relative concentration of the major analyte captured on the resin (e.g., for Run 2: Yb(III)-IDA_{DFOB}

= 0.79; and Cu(II)-IDA$_{BLM}$ = 0.88). Multiplication of the terms for resolution and capacity gives the PF for each resin type (e.g., for Run 2: Yb(III)-IDA$_{DFOB}$ = 1 × 0.79 = 0.79; and Cu(II)-IDA$_{BLM}$ = 0.77 × 0.88 = 0.68). A value of PF = 1 indicates an optimal resin type that enables the complete resolution of A1 from A2 and no loss of the target analyte in the unbound fraction. The overall performance factor (OPF) of a MD-IMAC system was defined in Equation 2 as the product of the two PF values for each resin type (e.g., for Run 2: 0.79 × 0.68 = 0.54).

$$PF = (1 - [A2]/[A1])([A1])\ldots\text{Eq. 1}$$

$$OPF = PF\ (\text{resin selecting [DFOB]>[BLM]}) \times PF\ (\text{resin selecting [BLM]>[DFOB]})\ldots\text{Eq. 2}$$

The resolution profile differed significantly when the column order was reversed (Cu(II)-charged IDA resin (upper), Yb(III)-charged IDA resin (lower)) (Fig. 2c,d). Under these conditions, DFOB was retained on the upper-positioned Cu(II)-charged IDA resin (80%), in addition to a significant fraction of BLM (41%) (Fig. 2d). This corroborated the earlier results (Fig. 1c,d), in which both analytes competed for sites on the upper-positioned Cu(II)-IDA resin.

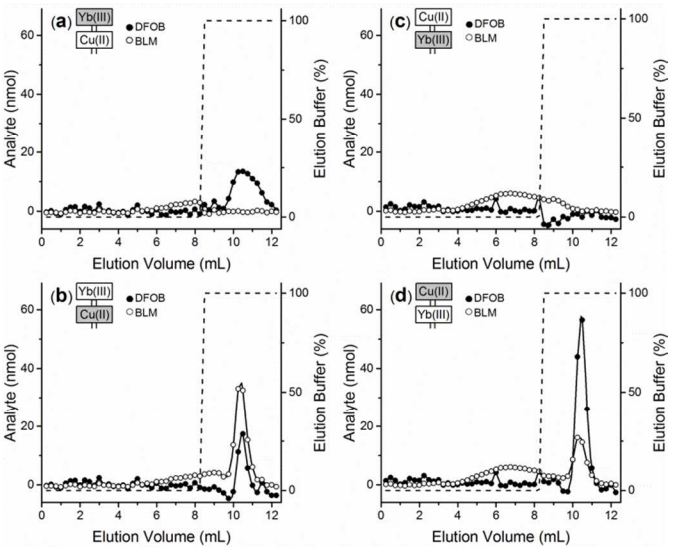

Fig. 2 The resolution profile of DFOB (closed circles) and BLM (open circles) upon processing an aliquot (250 µL) of an equimolar solution of DFOB and BLM (156 nmol:156 nmol) on two columns configured in series, which contained 1 mL of IMAC resin charged with Yb(III) (upper column, IDA resin) or Cu(II) (lower column, IDA resin) (**a**, **b**); or Cu(II) (upper column, IDA resin) or Yb(III) (lower column, IDA resin) (**c**, **d**). Analyte concentrations were measured in the fractions eluted with high-pH binding buffer from the two-column assembly, and from the individual columns with low-pH-5 elution buffer after disassembly (Yb(III), **a**, **c**; Cu(II), **b**, **d**). The gradient is shown as the broken line.

3.3. MD-IMAC for the resolution of BLM and DFOB from a standard solution: final experiments

The MD-IMAC format using a larger volume (2 mL) of Yb(III)-charged IDA resin in the upper-positioned column did not improve the resolution compared to the 1-mL system, with 64% DFOB adsorbed on the Yb(III)-charged resin and 29% DFOB on the Cu(II)-charged resin (Fig. S2). Further optimisation of the Yb(III)-based IMAC system for selecting DFOB examined the nature of the immobilised ligand. The higher coordination number (CN) preference of Yb(III) (CN 8-9) relative to more traditional IMAC metal ions (Ni(II), Cu(II), Co(II); CN 6), indicated that compared to tridentate IDA, the use of higher dentate immobilised ligands (e.g., pentadentate *N*,*N*,*N*′-tris(carboxymethyl)ethylenediamine (TED)) could simultaneously reduce metal leaching, due to the additional stability of the immobilised Yb(III)-pentadentate complex, and provide sufficient vacant sites (3-4) for target ligand binding. The log*K* value for the 1:1 complex between Yb(III) and pentadentate *N*′-benzylethylenediamine-*N*,*N*,*N*′-triacetic acid (BEDTRA) (log*K* 13.9),[41] supported the viability of an immobilised Yb(III)-pentadentate system for IMAC.

This concept was examined using a standard loading of DFOB (2.5 µmol) on four types of resin (1 mL): Ni(II)-charged IDA or COM (cOmplete resin (proprietary), containing a pentadentate ligand), and Yb(III)-charged IDA or COM. Similar to previous results,[5] the retention of DFOB on a 1-mL bed of Ni(II)-charged IDA resin was close to complete (Fig. 3a). In contrast, DFOB was not retained on the Ni(II)-charged COM resin, indicating that the single vacant site available on the immobilised Ni(II)-pentadentate complex was insufficient for binding (Fig. 3c). The resin remained blue-green in colour, consistent with the absence of Ni(II) leaching. While the majority of DFOB was not retained on the Yb(III)-charged IDA resin (Fig. 3b), due to exceeding the binding capacity, the entirety of the sample was retained on the Yb(III)-charged COM resin (Fig. 3d), which supported that by virtue of the higher CN preference of Yb(III), there remained sufficient sites available for DFOB binding. Elution of DFOB from the Yb(III)-COM resin required a greater volume (11 mL) of a low-pH EB at pH 4.0 (low-pH-4 EB), rather than pH 5.0 (low-pH-5 EB).

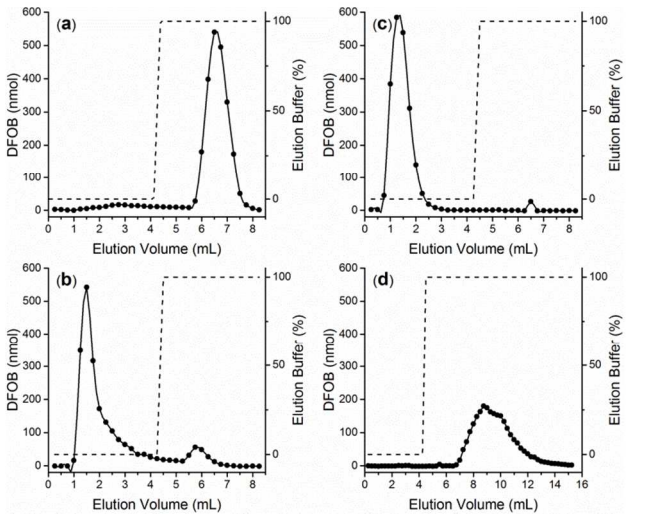

Fig. 3 The resolution profile from processing an aliquot of DFOB (2.5 µmol) on an IMAC column, which contained 1 mL of tridentate IDA resin charged with Ni(II) (**a**), or Yb(III) (**b**); or pentadentate COM resin charged with Ni(II) (**c**), or Yb(III) (**d**).

The gradient is shown as the broken line. Elution used low-pH-5 EB (**a**-**c**) or low-pH-4 EB (**d**).

Final experiments aimed to optimise BLM retention. The binding capacity of Cu(II)-IDA resin (~0.15-0.3 μmol mL^{-1}) towards BLM was greater than Cu(II)-NTA resin (<0.1 μmol mL^{-1}) (Fig. S3), which suggested that tridentate binding to form the ternary complex [Cu(II)(IDA)(BLM)] was the threshold requirement for BLM capture. BLM retention on Cu(II)-charged IDA resin (1 mL) was independent of incubation time (5 min versus 3 h) (Fig. S4). Other metal ions were examined for BLM binding, including In(III), which was selected based upon its classification as a borderline metal ion with a CN preference >6,[49] and studies of In(III)-BLM complexes as radio-pharmaceuticals.[50] BLM was not retained on either In(III)-charged IDA or NTA resins (Fig. S5). Due to the reactivity of Fe(II)-, Fe(III)- and Co(II)-BLM complexes,[51,52] these metal ions were not considered viable.

The complete set of optimisation experiments suggested that the most promising MD-IMAC format for resolving a solution of DFOB and BLM was Yb(III)-charged COM resin (upper column) and Cu(II)-charged IDA resin (lower column). This format provided a complete resolution of DFOB and BLM (Fig. 4a,b), with 93% of DFOB retained on the upper-positioned Yb(III)-COM resin (PF = 0.93) and 54% BLM on the lower-positioned Cu(II)-IDA resin (PF = 0.54), giving an OPF = 0.50.

Table 2 Concentration (% of loaded sample) of analytes DFOB and BLM resolved using a multi-dimensional IMAC format from a standard solution (STD), or from bacteriological medium with exogenous DFOB and BLM (MED), or from native *S. verticillus* culture supernatant (NAT)

RN	SMP[a]	Resin (U/L)[b]	Wash[c]	DFOB[d]	BLM[d]	PF[e]	OPF[f]	Fig
		BB	BB 8	10	96			1a,b
1	STD	Ni(II)-IDA (U)	EB 4	90	0	0.9	0.04	1a
		Cu(II)-IDA (L)	EB 4	0	4	0.04		1b
		BB	BB 8	20	31			1c,d
1R[g]	STD	Cu(II)-IDA (U)	EB 4	80	61	0.19	0.02	1d
		Ni(II)-IDA (L)	EB 4	0	8	0.08		1c
		BB	BB 8	1	12			2a,b
2	STD	Yb(III)-IDA (U)	EB 4	79	0	0.79	0.54	2a
		Cu(II)-IDA (L)	EB 4	20	88	0.68		2b
		BB	BB 8	20	46			2c,d
2R	STD	Cu(III)-IDA (U)	EB 4	80	41	0.39	0.05	2d
		Yb(III)-IDA (L)	EB 4	0	12	0.12		2c
		BB	BB 8	7	46			4a,b
3	STD	Yb(III)-COM (U)	EB 8	93	0	0.93	0.50	4a
		Cu(II)-IDA (L)	EB 4	0	54	0.54		4b
		BB	BB 8	8	54			4c,d
3R	STD	Cu(II)-IDA (U)	EB 4	92	44	0.48	0.01	4d
		Yb(III)-COM (L)	EB 8	0	2	0.02		4c
		BB	BB 4	13	4			5a,b
4	STD	Yb(III)-COM (U)	EB 8	87	0	0.87	0.84	5a
		Cu(II)-IDA (L)	EB 4	0	96	0.96		5b
		BB	BB 4	0	6			S7a,b
5	MED	Yb(III)-COM (U)	EB 8	100	0	1	0.94	S7a
		Cu(II)-IDA (L)	EB 4	0	94	0.94		S7b
		BB	BB 4	0	1			8a,b
6	NAT	Yb(III)-COM (U)	EB 8	100	0	1	0.99	8a
		Cu(II)-IDA (L)	EB 4	0	99	0.99		8b

[a] SMP, sample: STD, 156 nmol DFOB and 156 nmol BLM; MED, bacteriological medium containing 140 nmol DFOB and 140 nmol BLM; NAT, native *S. verticillus* culture supernatant. [b] Resin type (Position: U, upper; L, lower). [c] Experimental conditions (eg, for Run 1): after sample loading, the two-column assembly was washed with 8 mL of high-pH binding buffer (BB 8); following disassembly, individual columns were washed with 4 mL of low-pH elution buffer (EB 4). [d] Relative concentration (%) of DFOB or BLM. [e] PF, performance factor (refer Equation 1). [f] OPF, Overall performance factor (refer Equation 2). [g] R, reversed column order.

The reversal of column order did not afford any resolution, with both analytes concentrated on the upper-positioned Cu(II)-IDA resin (Fig. 4c,d). These data demonstrate that column order is a powerful determinant of the resolution of bacterial secondary metabolites in an MD-IMAC format. The fractionation of serum proteins has been examined using in-series columns containing several resin types[53-55] including Fe(III)- or Ni(II)-charged TED, which showed no difference in the separation profile as a function of column order.[53]

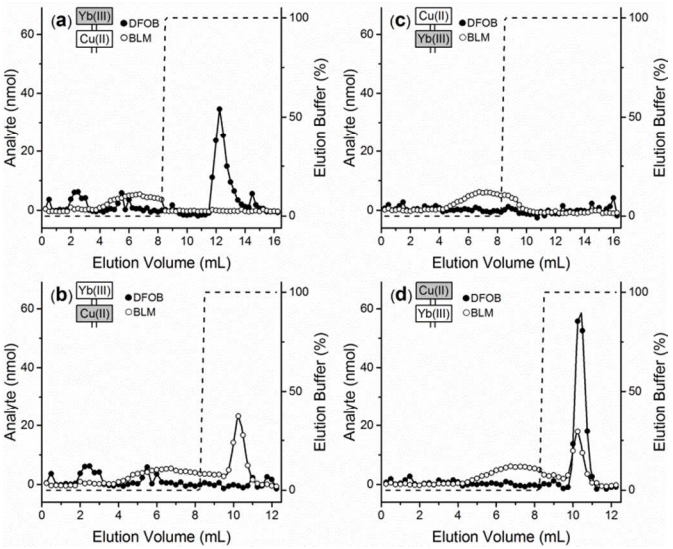

Fig. 4 The resolution profile of DFOB (closed circles) and BLM (open circles) upon processing an aliquot (250 µL) of an equimolar solution of DFOB and BLM (156 nmol:156 nmol) on two columns configured in series, which contained 1 mL of IMAC resin charged with Yb(III) (upper column, COM resin) or Cu(II) (lower column, IDA resin) (**a**, **b**); or Cu(II) (upper column, IDA resin) or Yb(III) (lower column, COM resin) (**c**, **d**). Analyte concentrations were measured in the fractions eluted with high-pH binding buffer from the two-column assembly, and from the individual columns with low-pH elution buffer after disassembly (Yb(III), low-pH-4 EB, **a**, **c**; Cu(II), low-pH-5 EB, **b**, **d**). The gradient is shown as the broken line.

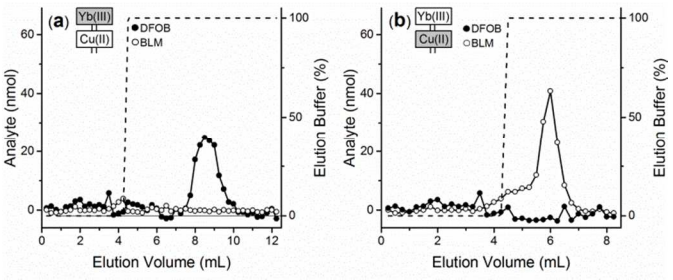

Fig. 5 The resolution profile of DFOB (closed circles) and BLM (open circles) upon processing an aliquot (250 µL) of an equimolar solution of DFOB and BLM (156 nmol:156 nmol) on two columns configured in series, which contained 1 mL of IMAC resin charged with Yb(III) (upper column, COM resin) or Cu(II) (lower column, IDA resin). Analyte concentrations were measured in the fractions (250 µL) eluted upon washing the two-column assembly with high-pH binding buffer (total volume 4 mL), and from the individual columns after disassembly with low-pH elution buffer (Yb(III), low-pH-4 EB (**a**); Cu(II), low-pH-5-EB (**b**)). The gradient is shown as the broken line.

The yield of BLM was lower than the yield observed in a similar single-column Cu(II)-IDA format, due to the extended washing with high-pH BB (8 mL) used for the 2-mL resin volume of the MD-IMAC format (Fig. S6). The reduction of the wash step to 4 mL in the MD-IMAC format (Fig. 5a,b) gave a profile that showed the complete resolution of DFOB and BLM, and the isolation of each analyte in good yield (DFOB, 87%; BLM, 96%), giving an OPF = 0.84.

3.4. Binding capacity of the Yb(III)-COM resin towards DFOB

The performance of the Yb(III)-charged pentadentate COM resin towards binding DFOB (Fig. 3-5) was superior to that of the tridentate IDA system (Fig. 2-3). Aside from its use in an MD-IMAC format, this new type of Yb(III)-charged IMAC resin could have utility in a single-column format for the isolation of DFOB and related siderophores from bacterial culture.[5,8]

In this context, the capacity of the Yb(III)-COM and Ni(II)-IDA resins towards binding ≥ 95% of a defined loading of DFOB was determined as 8 µmol mL^{-1} or 3.5 µmol mL^{-1}, respectively (Fig. 6, Table S1). The DFOB binding capacity of the Yb(III)-COM resin is about 2-fold greater than Ni(II)-IDA resin, which could be useful in the isolation of low-abundant bacterial siderophores and other secondary metabolites from culture. The increased binding capacity could result from a combination of the increased CN of Yb(III) and the higher ligand loading of the COM resin.

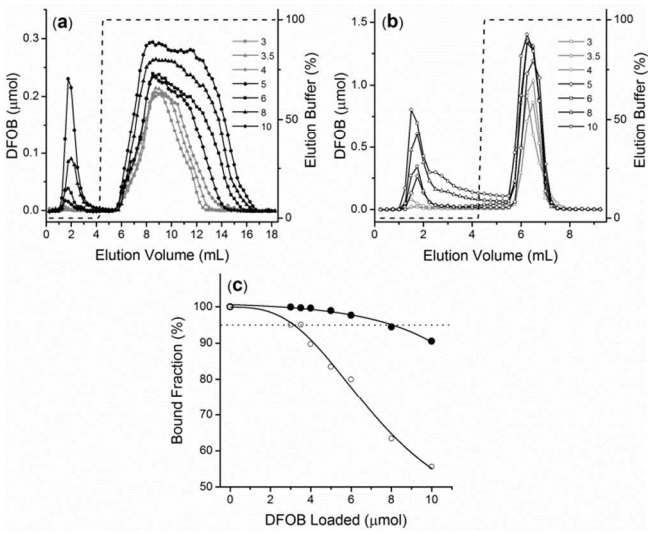

Fig. 6 The binding profiles of DFOB at loadings of 3, 3.5, 4, 5, 6, 8 or 10 µmol on 1 mL of (**a**) Yb(III)-COM resin; or (**b**) Ni(II)-IDA resin. DFOB concentrations were measured in the fractions (250 µL) eluted upon washing with high-pH binding buffer (total volume 4 mL), and with low-pH elution buffer (Yb(III), low-pH-4 EB; Ni(II), low-pH-5-EB). The gradient is shown as the broken line. Panel (**c**) shows the DFOB binding capacity of 1 mL of Yb(III)-COM (solid) or Ni(II)-IDA (open) resin, with the capacity defined as that which retained ≥ 95% DFOB (dotted).

3.5. MD-IMAC for the resolution of BLM and DFOB from native *S. verticillus* culture supernatant

S. verticillus culture supernatant (100 mL) harvested at day 10 was processed on XAD-2 resin to remove endogenous Cu(II) from native BLM. Analysis of this XAD-2-treated supernatant by LC-MS (TIC detection) showed a complex mixture containing medium components and secondary metabolites (Fig. 7a, solid). Since many *Streptomyces* species produce siderophores from the DFO class,[8,56-59] it was reasonable to assume that in addition to BLM, *S. verticillus* would biosynthesize DFOB and/or the macrocyclic analogue DFOE. The siderophore DFOB was detected using selected ion monitoring (SIM) detection at *m/z* 561 ($[M]^+$) and *m/z* 281 ($[M + H^+]^{2+}$) (Fig. 7a, inset, black). Supporting evidence for the assignment of this signal as DFOB was obtained from adding an aliquot of Fe(III) to the native culture, which resulted in the

disappearance of the peak at t_R 16.38 min (Fig. 7a, inset, gray), as consistent with the formation of Fe(III)-DFOB. There was no native DFOE detected in the culture (SIM at *m/z* 601). The presence of the two major BLM congeners, BLM A_2 and BLM B_2, was supported by the re-acquisition of the LC-MS trace following the addition of a solution containing authentic BLM and DFOB (Fig. 7a, dotted). This trace showed a relative increase in the signal intensity of two peaks at t_R 11.58 min and t_R 12.85 min, characteristic of the retention time of BLM A_2 and BLM B_2 (open circles).[6] The signal for exogenous DFOB eluted at a retention time (t_R 16.3 min, closed circle) that was co-incident with that for native DFOB, as detected using SIM (Fig. 7a, inset).

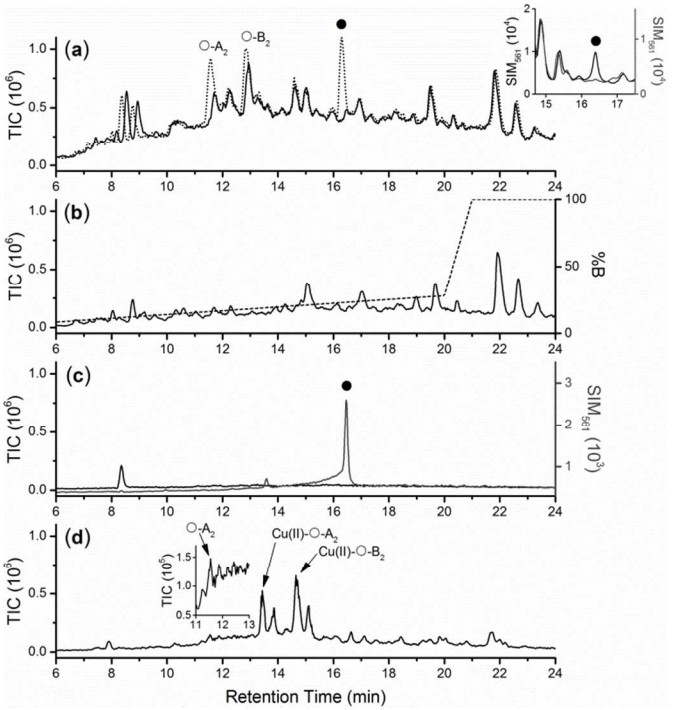

Fig. 7. LC-MS traces (detection: total ion counts (TIC)) from native *S. verticillus* culture supernatant following XAD-2 processing (**a**, solid), and with exogenous BLM A_2, BLM B_2 and DFOB (**a**, dotted). Inset: LC-MS trace (detection: SIM *m/z* 561) from native culture (solid), and with exogenous Fe(III) (gray). LC-MS traces (detection: TIC) from fractions collected from MD-IMAC processing of the native culture: unbound components (**b**); or components eluted from the Yb(III) (**c**, SIM *m/z* 561, gray), or the Cu(II) (**d**) resin. Signals due to BLM A_2, BLM B_2 or DFOB, are marked with ○-A_2, ○-B_2, or ●, respectively. The gradient (**b**, dotted) was the same in (**a**), (**c**) and (**d**).

The XAD-2-processed culture supernatant was freeze dried and dissolved in 1 mL of high-pH BB with pH adjustment to pH 9.0 required due to the acid present from the XAD-2-processing. The solution was subject to the optimised MD-IMAC system (Yb(III)-COM resin (upper column) and Cu(II)-IDA resin (lower column)), with fractions analysed by LC-MS using a combination of detection modes. The LC-MS trace from one fraction eluted from the two-column assembly during the high-pH BB wash showed that a significant proportion of species were removed (Fig. 7b). LC-MS traces from one fraction from the Yb(III)-COM resin as eluted after disassembly with low-pH-4 EB showed the presence of DFOB (Fig. 7c). Parallel analysis of one fraction from the Cu(II)-IDA resin showed that BLM was adsorbed onto the resin, and was eluted as a mixture of BLM A_2, Cu(II)-BLM A_2 and Cu(II)-BLM B_2 (Fig. 7d), indicating Cu(II) leaching from the Cu(II)-IDA resin. Two other signals at t_R 13.80 min ($[Cu(II)\text{-}M]^{2+}$, m/z_{obs} 744.2) and t_R 15.11 min ($[Cu(II)\text{-}M]^{2+}$, m/z_{obs} 749.8) were present in the LC-MS from this fraction, which were Cu(II)-BLM derived, but of uncertain nature.

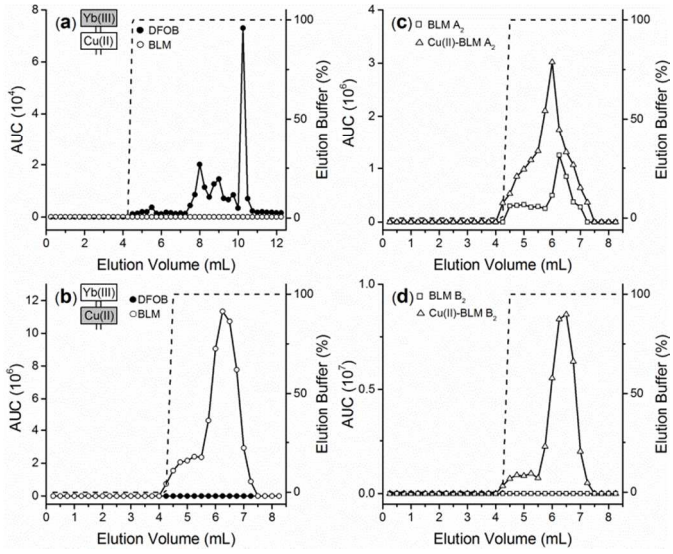

Fig. 8. The resolution profile of DFOB (closed circles) and BLM (open circles) upon processing an aliquot of native S. verticillus culture supernatant on two columns configured in series, which contained 1 mL of IMAC resin charged with Yb(III) (upper column, COM resin) or Cu(II) (lower column, IDA resin) (**a**, **b**). Analyte concentrations were measured as MS counts in the fractions eluted with high-pH binding buffer from the two-column assembly, and from the individual columns with low-pH elution buffer after disassembly (Yb(III), low-pH-4 EB, **a**; Cu(II), low-pH-5 EB, **b**). The gradient is shown as the broken line. The distribution of BLM A2 (open square) and Cu(II)-BLM A2 (open triangle) or BLM B2 (open square) and Cu(II)-BLM B2 (open triangle) is shown in (**c**) or (**d**), respectively.

Each fraction from the MD-IMAC experiment using native *S. verticillus* culture was subject to analysis by LC-MS. This resulted in a profile that showed the complete resolution of native DFOB and BLM from the complex *S. verticillus* secondary metabolome (Fig. 8, Table 2, Run 6). The binding profile of the DFOB from the Yb(III)-COM resin (Fig. 8a) was asymmetric, with the majority of DFOB eluted in the fraction at 10.25 mL. This asymmetry was likely attributed to a combination of very low levels of DFOB and the use of in-house-packed columns with heterogeneous resin beds. As determined from MS analysis, 100% of native DFOB was adsorbed onto the Yb(III)-COM resin (PF = 1), and 99% of native BLM was adsorbed onto the Cu(II)-IDA resin (PF = 0.99), with an OPF = 0.99. The absolute yields of both agents isolated from the native culture were unable to be accurately determined, but would be very low (ng-μg), which would be a factor that would positively influence the resolution. The DFOB was eluted from the resin as free ligand. The BLM was eluted from the Cu(II)-IDA column as a combination of free BLM A_2, Cu(II)-BLM A_2 and Cu(II)-BLM B_2. There was no BLM B_2 detected as free ligand, which suggested that BLM B_2

has a higher Cu(II) affinity compared to BLM A_2. An additional purification step involving XAD-2 chromatography would be required to remove Cu(II) from the Cu(II)-bound BLM species to produce BLM with potential for clinical use.

An additional MD-IMAC experiment was conducted using bacteriological medium that was not inoculated with *S. verticillus* and was processed using XAD-2 chromatography to which was added exogenous BLM (140 nmol) and DFOB (140 nmol). This experiment was conducted to verify the resolution of these agents in a model *S. verticillus* culture, and to allow for improved analyte detection. The resolution of BLM and DFOB in this model system was similar to that obtained for native culture, with 100% of DFOB retained on the Yb(III)-COM resin and 94% of BLM retained on the Cu(II)-IDA resin (Table 2, Run 5, Fig. S7). Due to the higher BLM loading in this experiment, the BLM was eluted as a combination of both congeners BLM A_2 and BLM B_2 as free ligands, together with the Cu(II) complexes. The absence of a peak front from the high-pH BB wash step in the elution profile of BLM B_2 (Fig. S7d) showed that this congener had a greater affinity towards the immobilised Cu(II)-IDA complex, compared to BLM A_2. Since the Cu(II) binding site is common between BLM A_2 and BLM B_2, this difference in affinity must arise from the strength of the interactions between the ancillary groups in BLM A_2 (aminopropyldimethylsulfonium) or BLM B_2 (agmatine) and the binary Cu(II)-IDA complex.

It was unclear whether the Cu(II) leaching by BLM was specific to the experiments involving bacteriological medium (inoculated and uninoculated) or whether this also occurred for standard BLM solutions. It was also important to verify the form of DFOB that was being eluted from the Yb(III)-COM resin. This was examined following the IMAC processing of loadings of standard solutions of BLM (156 nmol) or DFOB (156 nmol) on single 1-mL columns containing either Cu(II)-IDA or Yb(III)-COM resin (Fig. S8). LC-MS showed that DFOB was eluted as free ligand, and that BLM was eluted as a combination of free BLM A_2, Cu(II)-BLM A_2 and Cu(II)-BLM B_2. BLM-mediated Cu(II) leaching occurred under all the IMAC conditions examined here. The leaching could be exacerbated by the use of a low-pH EB, with potential for improvement with the use of imidazole-containing buffers. Each of these elution protocols would require a purification step downstream of single-column or MD-IMAC processing to either remove endogenous Cu(II) (low-pH EB) or excess imidazole (imidazole-containing buffer).

4. Conclusions

A standard solution of two clinical agents, DFOB and BLM, has been resolved using an IMAC format with two in-series columns containing Yb(III)-charged COM resin in the upper position (PF = 0.87) and Cu(II)-charged IDA resin (PF = 0.96) in the lower position, giving an OPF = 0.84. The resolution of DFOB and BLM was dependent upon the metal ion, the denticity of the immobilised chelate and the column order. The resolution arose due to the differential coordination chemistry of DFOB and BLM. A Yb(III)-charged COM (pentadentate) resin format has been described that has a DFOB binding capacity of 8 μmol mL^{-1}, which is more than 2-fold greater than the capacity of a previously described Ni(II)-IDA resin.[5] The performance of the Yb(III)-COM resin towards DFOB capture likely results in part from the increased number of binding sites available at the pentadentate complex arising from the expanded CN preference of Yb(III). The MD-IMAC method was used to resolve native DFOB and BLM from the culture of *S. verticillus*, which comprised a complex mixture of bacteriological medium components and other secondary metabolites.

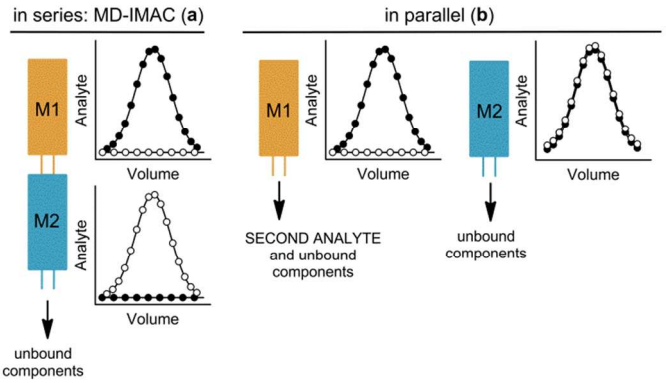

Scheme 3 The in-series column configuration of MD-IMAC resolved a mixture of DFOB (closed circle) and BLM (open circle) on individual columns (M1 = Yb(III)-COM, DFOB; M2 = Cu(II)-IDA, BLM) (**a**). Processing the same mixture on the same columns configured in parallel (**b**), would result in the isolation of DFOB on one column (M1 = Yb(III)-COM), with BLM co-eluting with other unbound components; and the co-adsorption of DFOB and BLM on the other column (M2 = Cu(II)-IDA), affording no resolution.

If the in-series MD-IMAC format (Scheme 3a) was re-configured to an in-parallel format (Scheme 3b), adsorption of a solution of DFOB and BLM would result in the selection of DFOB on the Yb(III)-charged IMAC resin, with BLM eluting as an unbound component, and the binding of both DFOB and BLM on the Cu(II)-charged IMAC resin, affording no resolution. This demonstrates the value of using an MD-IMAC format for the simultaneous resolution of clinical agents.

In this work, we have studied a two-column system, but the method could lend itself to an increased number of in-series columns to access more than two agents. This would likely lead to an enrichment of a given target on a column, rather than complete resolution, due to the increased likelihood of an overlap in the coordination chemistry preferences of each target.

Since IMAC and MD-IMAC experiments are easy to conduct and are water compatible, this technology could find use in streamlining pharmaceutics processing of bacterial metabolites obtained from fermentation. The utility of the method would be restricted to compounds with metal binding properties. With industry focus on improved Green chemistry processes for the delivery of active pharmaceutical ingredients (APIs),[60] it is timely to also consider improved Green chemistry

approaches for harvesting secondary metabolites from fermentation.

Acknowledgements

Receipt of an Australian Postgraduate Award (J.G.) and funding from The University of Sydney (R.C.) is gratefully acknowledged. Roche Diagnostics is kindly acknowledged for the provision of metal-free cOmplete His-Tag purification resin (COM).

School of Medical Sciences (Pharmacology) and Bosch Institute, The University of Sydney, New South Wales 2006, Australia.
† Electronic Supplementary Information (ESI) available: Fig. S1-S8; and Table S1 (as referenced in main article). See DOI: 10.1039/b000000x/

References

1 J. Porath, J. Carlsson, I. Olsson and G. Belfrage, *Nature*, 1975, **258**, 598-599.
2 E. S. Hemdan, Y.-J. Zhao, E. Sulkowski and J. Porath, *Proc. Natl. Acad. Sci. USA*, 1989, **86**, 1811-1815.
3 J. W. Wong, R. L. Albright and N.-H. L. Wang, *Sep. Purif. Rev.*, 1991, **20**, 49-106.
4 A. Charlton and M. Zachariou, in *Affinity Chromatography: Methods and Protocols*, ed. M. Zachariou, Humana Press, Totowa, 2008, vol. 421, pp. 137-149.
5 N. Braich and R. Codd, *Analyst*, 2008, **133**, 877-880.
6 J. Gu and R. Codd, *J. Inorg. Biochem.*, 2012, **115**, 198-203.
7 N. Ejje, E. Lacey and R. Codd, *RSC Adv.*, 2012, **2**, 333-337.
8 N. Ejje, C. Z. Soe, J. Gu and R. Codd, *Metallomics*, 2013, **5**, 1519-1528.
9 R. Codd, J. Gu, N. Ejje and T. Lifa, in *Inorganic Chemical Biology: Principles, Techniques and Applications*, ed. G. Gasser, John Wiley & Sons, Ltd, Chichester, UK, 2014, pp. 1-35.
10 K. L. Dunbar and D. A. Mitchell, *ACS Chem. Biol.*, 2013, **8**, 473-487.
11 D. J. Newman and G. M. Cragg, *J. Nat. Prod.*, 2012, **75**, 311-335.
12 J. M. Winter, S. Behnken and C. Hertweck, *Curr. Opin. Chem. Biol.*, 2011, **15**, 22-31.
13 R. M. Wilson and S. J. Danishefsky, *J. Org. Chem.*, 2006, **71**, 8329-8351.
14 B. B. Mishra and V. K. Tiwari, *Eur. J. Med. Chem.*, 2011, **46**, 4769-4807.
15 G. M. Cragg and D. J. Newman, *Biochim. Biophys. Acta*, 2013, **1830**, 3670-3695.
16 D. A. Dias, S. Urban and U. Roessner, *Metabolites*, 2012, **2**, 303-336.
17 P. Anastas and N. Eghbali, *Green Chem.*, 2010, **39**, 301-312.
18 A. Gałuszka, Z. Migaszewski and J. Namieśnik, *TrAC, Trends Anal. Chem.*, 2013, **50**, 78-84.
19 D. J. C. Constable, C. Jiménez-González and R. K. Henderson, *Org. Process Res. Dev.*, 2007, **11**, 133-137.
20 C. Jiménez-González, D. J. C. Constable and C. S. Ponder, *Chem. Soc. Rev.*, 2012, **41**, 1485-1498.
21 E. A. Peterson, B. Dillon, I. Raheem, P. Richardson, D. Richter, R. Schmidt and H. F. Sneddon, *Green Chem.*, 2014, **16**, 4060-4075.
22 B. A. Davis and J. B. Porter, in *Iron Chelation Therapy*, ed. C. Hershko, Kluwer Academic / Plenum Publishers, New York, 2002, pp. 91-125.
23 D. L. Boger and H. Cai, *Angew. Chem. Int. Ed.*, 1999, **38**, 448-476.
24 J. Chen and J. Stubbe, *Nat. Rev. Cancer*, 2005, **5**, 102-112.
25 B. La Ferla, C. Airoldi, C. Zona, A. Orsato, F. Cardona, S. Merlo, E. Sironi, G. D'Orazio and F. Nicotra, *Nat. Prod. Rep.*, 2011, **28**, 630-648.
26 H. Umezawa, K. Maeda, T. Takeuchi and Y. Okami, *J. Antibiot.*, 1966, **19**, 200-209.
27 C.-Y. Chen, S. Si, Q. He, H. Xu, M.-Y. Lu, Y. Xie, Y. Wang and R. Chen, *J. Antibiot.*, 2008, **61**, 747-751.
28 H. Umezawa, K. Maeda, Y. Okami and T. Takeuchi, 1972, US Patent 3,681,491.
29 H. Kawaguchi, H. Tsukiura, K. Tomita, M. Konishi, K. Saito, S. Kobaru, K. Numata, K. Fujisawa, T. Miyaki, M. Hatori and H. Koshiyama, *J. Antibiot.*, 1977, **30**, 779-788.
30 H. Bickel, *Helv. Chim. Acta*, 1963, **46**, 1385-1389.
31 V. Keri, Z. Czovek and A. Mezo, 2005, US Patent 6,858,414.
32 M. Chiani, A. Akbarzadeh, A. Farhangi, M. Mazinani, Z. Saffari, K. Emadzadeh and M. R. Mehrabi, *Pak. J. Biol. Sci.*, 2010, **13**, 546-550.
33 J. B. Neilands, *J. Am. Chem. Soc.*, 1952, **74**, 4846-4847.
34 H. Maehr, in *Antibiotics, Isolation, Separation, and Purification*, eds. M. J. Weinstein and G. H. Wagman, Elsevier Scientific Publishing Company, New York, 1978, vol. 15, pp. 521-585.
35 M. Zachariou, I. Traverso, L. Spiccia and M. T. W. Hearn, *J. Phys. Chem.*, 1996, **100**, 12680-12690.
36 M. J. Dilworth, K. C. Carson, R. G. F. Giles, L. T. Byrne and A. R. Glenn, *Microbiology*, 1998, **144**, 781-791.
37 A. E. Martell and R. M. Smith, *Critical Stability Constants*, Plenum Press, New York, 1974.
38 A. E. Martell and R. M. Smith, *Critical Stability Constants*, Plenum Press, New York, 1977.
39 Y. Sugiura, K. Ishizu and K. Miyoshi, *J. Antibiot.*, 1979, **32**, 453-461.
40 A. J. Bruno, S. Chaberek and A. E. Martell, *J. Am. Chem. Soc.*, 1956, **78**, 2723-2728.
41 J. H. Miller and J. E. Powell, *Inorg. Chem.*, 1978, **17**, 774-776.
42 R. Codd, *Coord. Chem. Rev.*, 2008, **252**, 1387-1408.
43 O. W. Duckworth, J. R. Bargar and G. Sposito, *Environ. Sci. Technol.*, 2009, **43**, 343-349.
44 A. Evers, R. D. Hancock, A. E. Martell and R. J. Motekaitis, *Inorg. Chem.*, 1989, **28**, 2189-2195.
45 R. G. Pearson, *J. Am. Chem. Soc.*, 1963, **85**, 3533-3539.
46 R. G. Pearson, *Coord. Chem. Rev.*, 1990, **199**, 403-425.
47 M. Zachariou, I. Traverso and M. T. Hearn, *J. Chromatogr.*, 1993, **646**, 107-120.
48 M. Zachariou and M. T. W. Hearn, *J. Chromatogr. A*, 2000, **890**, 95-116.
49 Y. Sun, C. J. Anderson, T. S. Pajeau, D. E. Reichert, R. D. Hancock, R. J. Motekaitis, A. E. Martell and M. J. Welch, *J. Med. Chem.*, 1996, **39**, 458-470.
50 A. D. Nunn, *Eur. J. Nucl. Med.*, 1977, **2**, 53-57.
51 J. N. Kemsley, K. L. Zaleski, M. S. Chow, A. Decker, E. Y. Shishova, E. C. Wasinger, B. Hedman, K. O. Hodgson and E. I. Solomon, *J. Am. Chem. Soc.*, 2003, **125**, 10810-10821.
52 J. C. Dabrowiak, *J. Inorg. Biochem.*, 1980, **13**, 317-337.

53 J. Porath and B. Olin, *Biochemistry*, 1983, **22**, 1621-1630.
54 J. Porath and P. Hansen, *J. Chromatogr.*, 1991, **550**, 751-764.
55 P. Samaraweera, J. Porath and J. W. Law, *Arch. Insect Biochem. Physiol.*, 1992, **20**, 243-251.
56 M. Imbert, M. Bechet and R. Blondeau, *Curr. Microbiol.*, 1995, **31**, 129-133.
57 A. A. Roberts, A. W. Schultz, R. D. Kersten, P. C. Dorrestein and B. S. Moore, *FEMS Microbiol. Lett.*, 2012, **335**, 95-103.
58 R. C. Hider and X. Kong, *Nat. Prod. Rep.*, 2010, **27**, 637-657.
59 V. H. Tierrafría, H. E. Ramos-Aboites, G. Gosset and F. Barona-Gómez, *Microb. Biotechnol.*, 2011, **4**, 275-285.
60 A. Larson and M. Meier, in *Green Techniques for Organic Synthesis and Medicinal Chemistry*, eds. W. Zhang and B. W. Cue, Jr, John Wiley & Sons, Ltd, Chichester, UK, 2012, pp. 573-587.